Original Research Article

EXTREME ULTRAVIOLET PENETRATION TO EARTH'S SURFACE: HUMAN AND ENVIRONMENTAL HEALTH IMPLICATIONS

ABSTRACT

Aims: Extreme ultraviolet radiation is widely believed to be completely absorbed by the atmosphere before reaching Earth's surface. Our objective is to make multiple measurements at Earth's surface of the solar irradiance spectrum in the range 200-400 nm.
Methods: We utilized International Light Technologies ILT950UV Spectral Radiometer mounted on a Meade LXD55 auto guider telescope tripod and mount assembly.
Results: Our multifold measurements of solar irradiance spectra demonstrate conclusively that all wavelengths in the spectral range 200-400 nm reach Earth's surface, contrary to the widespread perception that all UV-C and the majority of UV-B never reach the surface. We confirm the 2007 surface UV-C measurements of D'Antoni et al. that were disputed, based on faulty computer model calculations of atmospheric ozone, and thereafter ignored by the geoscience community.
Conclusions: The veracity our data and D'Antoni et al.'s data call into question the validity of atmospheric ozone models. Further, we call into question the simplistic supposition of the Montreal Protocol that chloro-fluoro-hydrocarbons are the primary cause of ozone depletion, and point to the very heavy burden of halogens introduced into the atmosphere by ongoing jet-sprayed coal-fly-ash geoengineering. We demonstrate that satellite-based LISIRD solar spectra irradiance at the top of the atmosphere is badly flawed with some regions of the spectrum being less intense than measured at Earth's surface. That calls into question any calculations made utilizing LISIRD data. We provide introductory information on the adverse effects of UV-B and UV-C on humans, phytoplankton, coral, insects and plants. These will be discussed in more detail in subsequent articles.

Keywords: Extreme ultraviolet, UV-C, UV-B, LISIRD, ozone depletion, ozone, ultraviolet damage, ultraviolet harm

1. INTRODUCTION

Geoengineering may be defined as the deliberate large-scale manipulation of the planetary environment including, but not limited to, dispersing particulate matter into the atmosphere to alter climate. Geoengineering experiments, conducted by the U. S. military and involving particulates emplaced into the atmosphere, go back at least to 1958 [1] and have continually increased in intensity and geographic range. About 2010, presumably through a secret international agreement, jet-spraying of particulates into the atmosphere became near-daily in intensity and near-global in range. The covert aerial particulate spraying was conducted without informed consent of those breathing the contaminated air, but with orchestrated false information, including in the scientific literature [2,3].

The geoscience community and the United Nation's Intergovernmental Panel on Climate Change, IPCC, has deceived the public and the scientific community by not taking into account the consequences of aerial particulate spraying on climate [4]. Even those who study the atmosphere do not mention the very-obvious aerial spraying, Figure 1.

Figure 1. Geoengineering aerosol particulate trails across the February 4, 2017 sky in Soddy-Daisy, TN (USA). With permission of David Tulis.

The typical geoscience presentation of the case for geoengineering is both simplistic and incorrect: In the future it may be necessary to place substances into the atmosphere to reflect away a portion of incident sunlight, 'sunshades for the Earth'; to compensate for supposed global warming presumably due to anthropogenic greenhouse gases, especially carbon dioxide. Placing particulate matter into the atmosphere not only reflects away a portion of incident sunlight, but also permits the particles to absorb radiant solar energy and transfer it to the atmosphere by molecular collisions. Furthermore, emplaced particulate aerosols retard infrared heat loss from Earth's surface and impede rainfall by preventing moisture droplets from coalescing to become massive enough to fall as rain. Eventually, the atmosphere becomes so moisture-saturated that it results in abnormal downpours, storms, and flooding. In short, the aerial particulate emplacement has a net effect of causing global warming and disrupting normal hydrological cycles.

Moreover, as described below (and in subsequent articles in this series), ongoing geoengineering may be causing a disruption of the ozone layer, endangering all life.

Though the geoscience community ignores the aerosol particulate spraying, there are many millions of ordinary citizens who harbor legitimate concerns about the activity [5]. Some individuals have taken rainwater samples and had them analyzed by commercial laboratories. Usually aluminum analyses have been requested; sometimes aluminum and barium; and rarely, aluminum, barium and strontium. We had rain and snow samples analyzed for a greater number of elements and showed that the elements thus determined were consistent with coal fly ash as the main aerosolized substance used in ongoing geoengineering operations [6-10].

When coal is burned by electric utilities the heavy ash settles and the light ash, called coal fly ash (CFA), forms and accumulates in the hot gases above the burner. Unless trapped and sequestered, the CFA exits the utilities' smokestacks. CFA contains a concentration of the toxic elements found in coal, including arsenic, chromium, thallium, and radioactive elements, to name a few. CFA also contains environmentally harmful elements such as mercury and chlorine. For public and environmental health reasons CFA is typically trapped and stored in Western nations.

Why would CFA be sprayed into the atmosphere for geoengineering purposes? CFA is one of the world's largest industrial waste streams with approximately 160 million tons generated annually in the U.S. [11], and approximately 750 million tons generated annually worldwide [12]. Little additional processing is necessary for this abundantly available and inexpensive waste product to be utilized in aerosol geoengineering operations as CFA particles typically form in the size range 0.1 – 50 µm [13]. Worldwide availability, low cost, and in-place production and storage facilities at coal-burning utilities

all contribute to making CFA an attractive aerosol geoengineering material. Though CFA is no longer regulated as a hazardous waste by the U.S. EPA, it is nonetheless toxic to most biota and, as discussed below, disrupts the atmospheric integrity that makes life possible on Earth.

Life on Earth depends critically on natural processes that shield it from the relentless hazardous onslaught of solar radiation. The first line of defense is the geomagnetic field that deflects the brunt of the sun's charged particles safely around Earth [14]. Our atmosphere is the second line of defense that protects life from solar ultraviolet radiation. Plants and animals on Earth are shielded from harmful solar radiation by our planet's stratospheric ozone layer, which is thought to form from the interaction of ultraviolet radiation with O_2, which is produced and sustained by photosynthesizing organisms. On numerous occasions the assertion has been made that no UV-C radiation (100-290 nm) reaches Earth's surface [15-17]. Here we dispute that assertion, using spectrometric measurements that indicate the probable debilitation of Earth's biota caused by the levels of UV-C radiation we recorded over the course of one year.

Ozone, O_3, and atmospheric oxygen, O_2, are widely thought to prevent over 90% of the UV-B radiation (290-320 nm) and all of the UV-C radiation (100-290 nm) from reaching Earth's surface. For the past three decades the geoscience community has focused on ozone depletion in connection with the so-called Antarctic 'ozone hole', and held to the theory, adopted by the 1987 Montreal Protocol, that fluoro-chloro-hydrocarbons (CFCs) are primarily responsible for the destruction of ozone through atmospheric reactions that produce ozone-destroying chlorine. Here we dispute that theory and recommend that other sources for ozone depletion should be considered, notably including CFA aerosol geoengineering.

2. METHODS

The experimental method employed pertains to solar spectrometric irradiance measurements at Earth's surface. This is a new line of investigation employing International Light Technologies ILT950UV Spectral Radiometer with fractional-nanometer resolution in the short-wavelength portion of the ultraviolet (UV) spectrum. The initial order to International Light Technologies specified that solar radiation measurements were to be performed with this unit, and that power levels to be measured in $\mu W/cm^2/nm$. International Light Technologies provided all training, and feedback analysis of initial data gathered to insure correct measurement process. The ILT950UV Spectral Radiometer was certified to ISO 17025.

The measurement process is as follows: The sensor for the ILT950UV is attached to a bracket located on the forward ring mount of the Meade LXD55 auto guider telescope tripod and mount assembly. The ILT950UV Spectral Radiometer is form fitted with foam rubber and installed inside the mount rings. The sensor and Radiometer are attached via fiber optic cable. This telescope mount is then set to the current latitude, oriented true North, programmed with current date and time, and then allowed to complete a calibration sequence. Post completion of this calibration, Sol is selected and entered. The telescope mount automatically tracks to Sol, and provides an accuracy of +/- 50 arc seconds relative to Sol. This automatic tracking of Sol mitigates the addition of "Sigma" phase error mathematical corrections.

The ILT950UV is then attached to a laptop computer with the software provided by International Light Technologies. A USB cable is attached from the laptop computer and the ILT950UV. The assembly is shown in Figure 2.

Figure 2. Spectrometer system.

The International Light Technologies software Program is initialized using “Administrator” privileges to ensure primary communication via the USB interface. The dark cap is installed over the sensor on the telescope mount, and the ILT950UV software calibration procedure begins with selecting the calibration file supplied by International Light Technologies, under the “SETUP” function tab.

Under the “ACQUIRE” tab, the Integration time is set to 10 milliseconds, and the SCAN AVERAGE is set to 100. The integration time is much like setting the exposure level on a camera, and was selected for “best fit” of high and low irradiance levels, keeping within the dynamic range of the radiometer. The SCAN AVERGE of 100 allows higher repeatability.

Next, a “DARK SCAN” is performed with the dark cap placed over the sensor, the ILT950UV “Dark Scan” is selected under the “Acquire” tab, and when complete responds with a “green” “DARK: ON” (background color of the cell) indication at the bottom center left of the computer display notifying the user the dark reference is valid.

The dark cap over the sensor is removed, and under the “Acquire” tab a “Reference Scan” is selected, once complete the ILT950UV validates with a “green” “REF: ON” indication at the bottom center right of the computer display.

Once the Dark and Reference scans are complete, the “Timeline” is selected under the “Acquire” tab. Within the GUI that is displayed there is a calendar and time start/stop setting, the interval setting, and how the data is to be exported to a file.

Solar position angles relative to the measurement geophysical location determine the length of the data recording session, with winter months being the shortest of 3 to 4 hours, and summer the longest with up to 6 hours.

The “Timeline” is set and the interval is set to 2 seconds. This provides a complete spectral scan from 200 to 450 nanometers every 2 seconds, and results in 1,854 data points gathered from 200 to 450nm in 1 scan, to be repeated every 2 seconds.

The “Export as Excel file” button is selected with “TimelineBY_” preceding the date and time code information of each filename used.

Once the “Start” and “Stop” entries are made, the “Begin” button is activated which starts the Spectral Radiometer scans.

3. RESULTS AND DISCUSSION

The two curves in Figure 3 present typical examples of the spectrometric data obtained using the ILT950UV in the manner described above at 10:49a local time on June 17, 2017 (black curve) at location (37.517783, -120.856783), elevation 56 m and at 12:21p local time on January 20, 2018 (red curve) at the same location. Clearly the spectral irradiances extend throughout the entire ultraviolet (UV) spectrum (200–400 nm) shown. Generally, for purposes of discussion the UV spectrum is divided into three parts, UV-A, UV-B, and UV-C, although some variation exists in wavelength specifications of those divisions. Here we use vertical dashed lines to indicate one set of divisions.

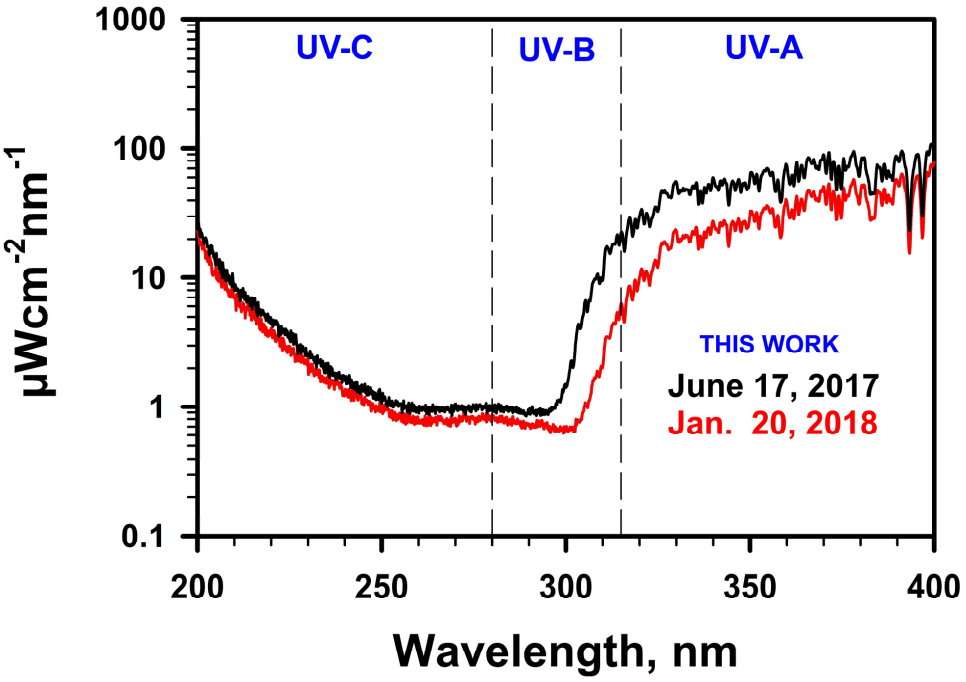

Figure 3. Examples of our solar spectral irradiance measurements.

There are widespread assertions in the medical, public health, and geoscience literature that no UV-C reaches the surface and only a portion of the UV-B does so [17-21]. Figure 4 shows our solar spectral irradiance measurements from Figure 3 together with two solar irradiance spectra measured at latitudes 38°S (green curve) and 38°N (pink curve) as reported in 2002 [22]. Close inspection of the figure reveals that the 38°S green curve has higher resolution than the 38°N pink curve, but, more importantly, our red and black curves have even higher resolution than the 38°S green curve. Our higher resolution is particularly important when one notices the major difference in those curves: All of our UV-B and all of our UV-C measurements are non-zero, quite unlike the widespread and incorrect assumption [17-21].

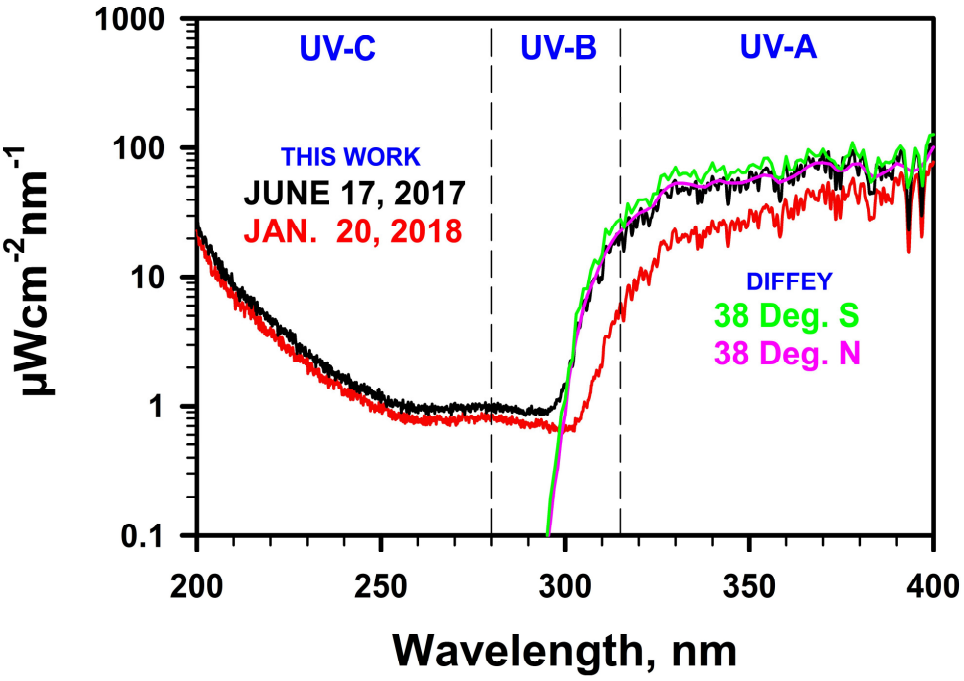

158

159 **Figure 4.** Comparison of our solar spectral irradiance measurements with those of Diffey [22].

160 For more than four decades, the geoscience community has increasingly functioned on the basis of
161 committee/political standards rather than long-held scientific standards [23]. When an important
162 contradiction arises in science, scientists have an obligation to attempt to ascertain the veracity of the
163 contradiction and, if warranted, to correct the contradicted former understanding.

164 In 2007 D'Antoni et al. [24] published spectral irradiance measurements made on two mountain
165 slopes in Tierra del Fuego, Argentina with elevations ranging 245-655 m. All of their published results
166 showed detected radiation in the UV-C region. Figure 5 compares our measured solar spectral
167 irradiance measurements from Figure 3 with published spectral irradiance measurements of D'Antoni
168 et al. [24].

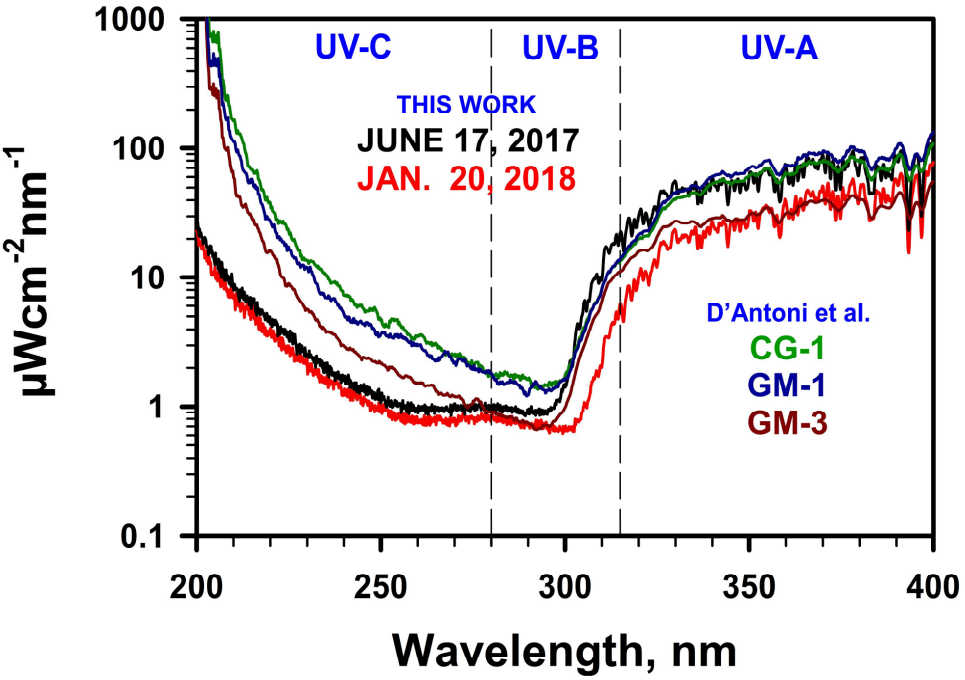

Figure 5. Comparison of our solar spectrometric measurements with those of D'Antoni et al. [24]. Note the commonality of shape of the curves in the UV-C region of the spectrum.

In Figure 5 we provide confirmatory evidence of the veracity of D'Antoni et al.'s measurements, which in turn confirms our own measurements. Independently, solar UV-C radiation was detected at Earth's surface using a fundamentally different methodology, employing a KCl:Eu2+ dosimeter [25,26]. That independent detection of UV-C irradiance stands as evidence that our UV-C measurements and D'Antoni et al.'s UV-C measurements were not the result of spurious spectrometer-generated artifacts.

In 2008 Flint et al. [27] published a response to D'Antoni et al. [24] in which they claimed the measurements were without merit, to which D'Antoni et al. [28] replied. Flint et al. asserted that ozone model calculations ruled out UV-C reaching Earth's surface, therefore the spectrometer must have been defective. Based upon the data shown in Figure 5, clearly the model calculations of atmospheric ozone were wrong.

Models are not science, they are computer programs that typically begin with a known end result and achieve that end result by making selective assumptions and parameter choices. During the last four decades computer-model calculations have burgeoned. It is far easier to make models than to make basic scientific discoveries, and it is the latter, not the former, that are fundamental to scientific progress [29].

In Figure 6 we show our Earth surface solar spectral irradiance data from Figure 3 compared with LISIRD satellite-derived solar spectral irradiance at the top of the atmosphere [30], indicated by the green curve for each of the two dates which are coincident. With satellite-data sets such as this it is difficult to know whether the data is raw or altered based upon models or assumptions. Clearly, there is a problem when the measured ground-level solar UV-C irradiance exceeds that at the top-of-atmosphere.

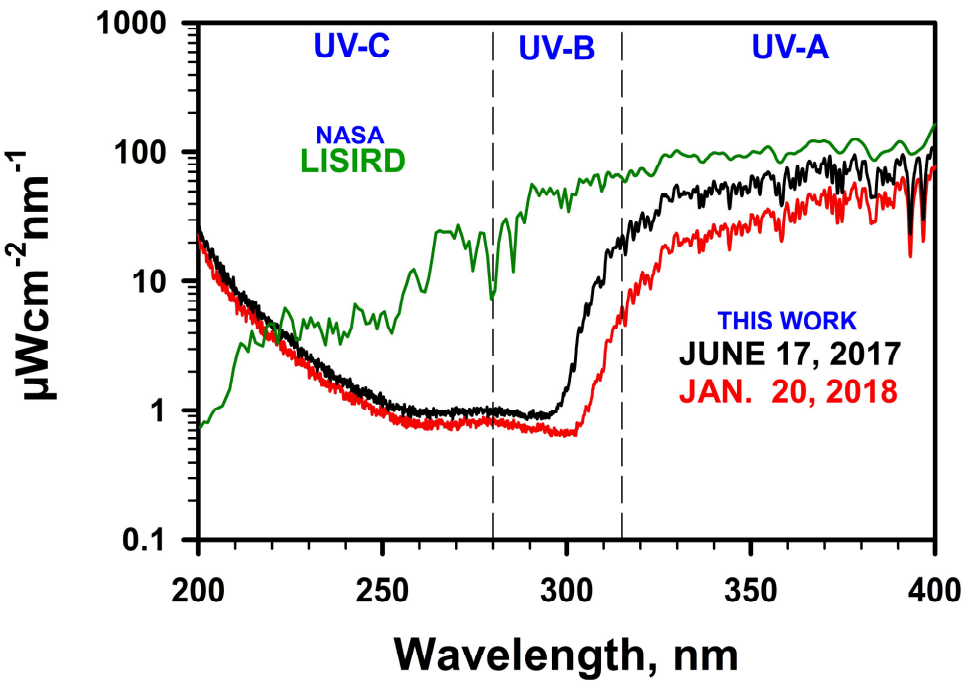

194

195 **Figure 6.** Comparison of our UV solar spectral irradiance with NASA's LISIRD satellite-derived solar
196 spectral irradiance at the top of the atmosphere [30].

197 The consensus-approved, model-driven solar irradiance storyline is badly flawed with regard to ozone
198 viability and perceived threats to ozone depletion. UV-C and all of UV-B radiation reach Earth's
199 surface where they pose potentially serious environmental and human health problems. The Montreal
200 Protocol prohibition of CFCs does not begin to address the life-threatening problems posed by other
201 sources of ozone-destroying chemicals. Table 1 shows the range of halogen compositions of coal fly
202 ash (CFA). Covert geoengineering that jet sprays massive quantities of ultra-fine CFA potentially
203 places vast amounts of chlorine, bromine, fluorine and iodine into the atmosphere all of which can
204 deplete ozone. Potentially other substances in CFA aerosols, including nano-particulates, might
205 adversely affect atmospheric ozone.

206

207 **Table 1.** Range of halogen element compositions of CFA [31]

Chlorine µg/g	Bromine µg/g	Fluorine µg/g	Iodine µg/g
13 – 25,000	0.3 – 670	0.4 – 624	0.1 – 200

208

Ultraviolet radiation is the most harmful and genotoxic component of the solar radiation spectrum. The mutagenicity and lethal action of sunlight exhibit two maxima, both in the UV region of the spectrum. This is because DNA bases can directly absorb incident UV photons of certain wavelengths. Solar radiation can give rise to cellular DNA damage by either (1) direct excitation of DNA (UV-B and UV-C) or (2) indirect mechanisms that involve excitation of other cellular chromophobes acting as endogenous photosensitizers (UV-A) [32]. The direct excitation of DNA generates predominantly cyclobutane pyrimidine dimers and photoproducts, which are of principal importance for the cytotoxic, mutagenic, and carcinogenic effects of short-wave UV radiation (UV-B and UV-C) [33]. Some of the most hazardous UV radiations have wavelengths between 240 and 300 nm. In this range, the wavelength with the minimum TLV (threshold limit value), or most hazardous, is around 270 nm [34].

UV-B radiation is a global stressor with potentially far-reaching ecological impacts. A meta-analysis of UV radiation on marine and freshwater organisms found large negative (but variable) effects of UV-B on survival and growth of organisms that crossed life histories, trophic groups, habitats, and life history stages [35]. In phytoplankton and zooplankton, increased levels of UV-B can affect photosynthesis, decrease growth and metabolic rates, impair nitrogen assimilation, impair motility, and bleach photopigments [36]. Extreme UV-B radiation is damaging to coral reef communities and associated with coral bleaching processes [37]. Corals accidentally exposed to UV-C showed gastrodermal cell death and necrosis resulting in the release of intracellular zoo-xanthellae into the gastrovascular canals and water column, likely resulting in a bleaching effect [38].

Enhanced UV-B radiation reduces genome stability in plants [39]. Enhanced UV radiation affects trees by direct action and modification of their biological/chemical environment (Figure 7). A recent study documents that high UV-B intensity leads to defective pollen development in conifers and decreased reproductive success or even sterilization [40].

Figure 7. July 21, 2017 photo of tree in New York, NY (USA) showing UV burn and concomitant fungal growth on sun-exposed side.

The toxicity of UV-C (100-280 nm) is well known. UV-C irradiation has lethal effects on insects and microorganisms [41,42]. UV-C radiation induces programmed cell death, or apoptosis, in plant cells [43]. In a controlled study, numerous ultrastructural changes and associated cell damage were shown in mole rat kidney tissue cells irradiated with artificially produced UV-C radiation [44]. Medical students accidentally exposed for 90 minutes to UV-C radiation from a germicidal lamp all suffered reversible photokeratitis, and skin damage to the face, scalp, and neck [45].

4. CONCLUSION

Measurement of solar irradiance spectra in the range 200-400 nm demonstrates conclusively that all wavelengths in that spectral range reach Earth's surface, contrary to the widespread perception that all UV-C and the majority of UV-B never reaches the surface. We confirm the 2007 surface UV-C measurements of D'Antoni et al. that were disputed, based on faulty computer model calculations of atmospheric ozone, and thereafter ignored by the geoscience community. The veracity of D'Antoni et al.'s data call into question the validity of atmospheric ozone models. Further, we call into question the simplistic supposition of the Montreal Protocol that CFCs are the primary cause of ozone depletion, and point to the very heavy burden of halogens introduced into the atmosphere by ongoing jet-sprayed coal-fly-ash geoengineering. We demonstrate that LISIRD solar spectra irradiance at the top of the atmosphere is badly flawed with some regions of the spectrum being less intense than measured at Earth's surface. That calls into question any calculations made utilizing LISIRD data. We provided introductory information on the adverse effects of UV-B and UV-C on humans, phytoplankton, coral, insects and plants. These will be discussed in more detail in subsequent articles.

REFERENCES

1. http://www.nuclearplanet.com/1958evidence.pdf

2. Shearer C, West M, Caldeira K, Davis SJ. Quantifying expert consensus against the existence of a secret large-scale atmospheric spraying program. Environ Res Lett. 2016;11(8):p. 084011.

3. Tingley D, Wagner G. Solar geoengineering and the chemtrails conspiracy on social media. Palgrave Communications. 2017;3(1):12.

4. Herndon JM. An open letter to members of AGU, EGU, and IPCC alleging promotion of fake science at the expense of human and environmental health and comments on AGU draft geoengineering position statement. New Concepts in Global Tectonics Journal. 2017;5(3):413-6.

5. http://wwwnuclearplanetcom/websites.pdf

6. Herndon JM. Aluminum poisoning of humanity and Earth's biota by clandestine geoengineering activity: implications for India. Curr Sci. 2015;108(12):2173-7.

7. Herndon JM. Obtaining evidence of coal fly ash content in weather modification (geoengineering) through analyses of post-aerosol spraying rainwater and solid substances. Ind J Sci Res and Tech. 2016;4(1):30-6.

8. Herndon JM. Adverse agricultural consequences of weather modification. AGRIVITA Journal of agricultural science. 2016;38(3):213-21.

9. Herndon JM, Whiteside M. Further evidence of coal fly ash utilization in tropospheric geoengineering: Implications on human and environmental health. J Geog Environ Earth Sci Intn. 2017;9(1):1-8.

10. Herndon JM, Whiteside M. Contamination of the biosphere with mercury: Another potential consequence of on-going climate manipulation using aerosolized coal fly ash J Geog Environ Earth Sci Intn. 2017;13(1):1-11.

11. Yao Z, Ji X, Sarker P, Tang J, Ge L, Xia M, et al. A comprehensive review on the applications of coal fly ash. Earth-Science Reviews. 2015;141:105-21.

12. Izquierdo M, Querol X. Leaching behavior of elements from coal combustion fly ash: an overview. Int J Coal Geol. 2012;94:54-66.

13. Chen Y, Shah N, Huggins F, Huffman G, Dozier A. Characterization of ultrafine coal fly ash particles by energy filtered TEM. Journal of Microscopy. 2005;217(3):225-34.

14. Parker E. Interaction of the solar wind with the geomagnetic field. The Physics of Fluids. 1958;1(3):171-87.

15. Frederick J, Snell H, Haywood E. Solar ultraviolet radiation at the earth's surface. Photochemistry and photobiology. 1989;50(4):443-50.

16. Pinedo-Vega JL, Ríos-Martínez C, Navarro-Solís DJ, Dávila-Rangel JI, Mireles-García F, Saucedo-Anaya SA, et al. Attenuation of UV-C Solar Radiation as a Function of Altitude (0≤ z≤ 100 km): Rayleigh Diffusion and Photo Dissociation of O2 Influence. Atmospheric and Climate Sciences. 2017;7(04):540.

17. Wilson BD, Moon S, Armstrong F. Comprehensive review of ultraviolet radiation and the current status on sunscreens. The Journal of clinical and aesthetic dermatology. 2012;5(9):18.

18. Seebode C, Lehmann J, Emmert S. Photocarcinogenesis and skin cancer prevention strategies. Anticancer research. 2016;36(3):1371-8.

19. Stapleton AE. Ultraviolet radiation and plants: burning questions. The Plant Cell. 1992;4(11):1353.

20. https://www.cdc.gov/healthyyouth/skincancer/pdf/qa.pdf

21. http://www.who.int/uv/faq/whatisuv/en/index2.html

22. Diffey BL. Sources and measurement of ultraviolet radiation. Methods. 2002;28(1):4-13.

23. Herndon JM. Corruption of Science in America. The Dot Connector. 2011. http://www.nuclearplanet.com/corruption.pdf

24. D'Antoni H, Rothschild L, Schultz C, Burgess S, Skiles J. Extreme environments in the forests of Ushuaia, Argentina. Geophysical Research Letters. 2007;34(22).

25. Córdoba C, Munoz J, Cachorro V, de Carcer IA, Cussó F, Jaque F. The detection of solar ultraviolet-C radiation using KCl:Eu2+ thermoluminescence dosemeters. Journal of Physics D: Applied Physics. 1997;30(21):3024.

26. de Cárcer IA, Dántoni H, Barboza-Flores M, Correcher V, Jaque F. KCl: Eu2+ as a solar UV-C radiation dosimeter. Optically stimulated luminescence and thermoluminescence analyses. Journal of Rare Earths. 2009;27(4):579-83.

27. Flint SD, Ballaré CL, Caldwell MM, McKenzie RL. Comment on “Extreme environments in the forests of Ushuaia, Argentina” by Hector D'Antoni et al. Geophysical Research Letters. 2008;35(13).

28. D'Antoni HL, Rothschild LJ, Skiles J. Reply to comment by Stephan D. Flint et al. on “Extreme environments in the forests of Ushuaia, Argentina”. Geophysical Research Letters. 2008;35(13).

29. Herndon JM. Geodynamic Basis of Heat Transport in the Earth. Curr Sci. 2011;101(11):1440-50.

30. LISIRD Data Systems Group, 2017, LASP Interactive Solar Irradiance Dataset, http://lasp.colorado.edu/lisird/lya/

31. NRC. Trace-element Geochemistry of Coal Resource Development Related to Environmental Quality and Health: National Academy Press; 1980.

32. Ravanat J-L, Douki T, Cadet J. Direct and indirect effects of UV radiation on DNA and its components. Journal of Photochemistry and Photobiology B: Biology. 2001;63(1):88-102.

33. Kielbassa C, Roza L, Epe B. Wavelength dependence of oxidative DNA damage induced by UV and visible light. Carcinogenesis. 1997;18(4):811-6.

34. http://www2.lbl.gov/ehs/safety/nir/ultraviolet_radiation.shtml

35. Bancroft BA, Baker NJ, Blaustein AR. Effects of UVB radiation on marine and freshwater organisms: a synthesis through meta-analysis. Ecology letters. 2007;10(4):332-45.

36. El-Sayed SZ, Van Dijken GL, Gonzalez-Rodas G. Effects of ultraviolet radiation on marine ecosystems. International Journal of Environmental Studies. 1996;51(3):199-216.

37. Lyons M, Aas P, Pakulski J, Van Waasbergen L, Miller RV, Mitchell D, et al. DNA damage induced by ultraviolet radiation in coral-reef microbial communities. Marine Biology. 1998;130(3):537-43.

38. Basti D, Bricknell I, Beane D, Bouchard D. Recovery from a near-lethal exposure to ultraviolet-C radiation in a scleractinian coral. Journal of invertebrate pathology. 2009;101(1):43-8.

39. Ries G, Heller W, Puchta H, Sandermann H, Seidlitz HK, Hohn B. Elevated UV-B radiation reduces genome stability in plants. Nature. 2000;406(6791):98.

40. Benca JP, Duijnstee IA, Looy CV. UV-B–induced forest sterility: Implications of ozone shield failure in Earth's largest extinction. Science Advances. 2018;4(2):e1700618.

41. Hori M, Shibuya K, Sato M, Saito Y. Lethal effects of short-wavelength visible light on insects. Scientific Reports. 2014;4:7383.

42. Reed NG. The history of ultraviolet germicidal irradiation for air disinfection. Public health reports. 2010;125(1):15-27.

43. Danon A, Gallois P. UV-C radiation induces apoptotic-like changes in Arabidopsis thaliana. FEBS letters. 1998;437(1-2):131-6.

395 44. Türker H, Yel M. Effects of ultraviolet radiation on mole rats kidney: A histopathologic and
396 ultrastructural study. Journal of Radiation Research and Applied Sciences. 2014;7(2):182-7.

397

398 45. Trevisan A, Piovesan S, Leonardi A, Bertocco M, Nicolosi P, Pelizzo MG, et al. Unusual High
399 Exposure to Ultraviolet-C Radiation. Photochemistry and photobiology. 2006;82(4):1077-9.